DTIC
SELECTED
DEC 2 3 1994
F

Performance Modeling of Hyperspectral Imaging Sensors
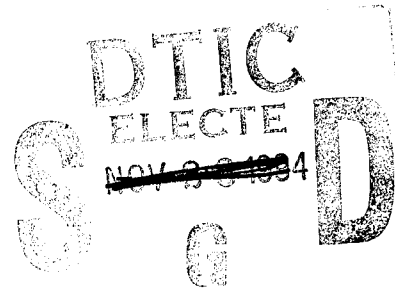## for Atmospheric Studies

Grant No. N00014-94-1-6004
G-004

from

Naval Research Laboratory
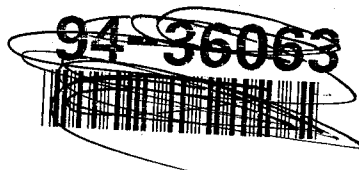Washington, D.C.

Final Technical Report

DTIC
ELECTE
NOV 1994
S   G   D

Yudi Adityawarman
R. A. Schowengerdt
Department of Electrical and Computer Engineering
University of Arizona
Tucson AZ 85721

9   19941219 079

September, 1994

DTIC QUALITY INSPECTED 5

94-36063

Contents 2

EXECUTIVE SUMMARY

In this research project, we have developed a sensor model for the Navy's HYDICE system, using current engineering specifications and data from Hughes Danbury Optical Systems, the manufacturer. This sensor imaging model has been integrated into an end–to–end simulation system, Multispectral Image Simulator (MIS). Using MIS with the HYDICE model we have investigated Signal–to–Noise Ratios (SNRs) that might be expected from HYDICE under low radiance conditions, such as images of coastal water areas. The results are presented in Section 4.1. We also used the Cuprite, Nevada, AVIRIS database developed earlier, for simulation of natural HYDICE imagery. This is presented in Section 4.2. Finally, we have also initiated investigation of large view angle effects on image contrast, using the Advanced Very High Resolution Radiometer (AVHRR) module in MIS since it allows a range of ±55° in view angle cross–track. These simulation results are presented in Section 4.3.

The HYDICE SNR and AVHRR view angle simulations are done with a sinusoidal reflectance input target. This permits variation of the frequency of the target to model sensor MTF effects, variation of the amplitude of the target to model scene contrast, and variation of the mean level to model absolute reflectance level. The results therefore condense a large amount of atmospheric/sensor parametric information into a usable engineering form.

Accesion For		
NTIS CRA&I	☐	
DTIC TAB	☐	
Unannounced	☐	
Justification		
By		
Distribution /		
Availability Codes		
Dist	Avail a d / or Special	

1.0 INTRODUCTION

Recently increased interest in monitoring global changes in the earth's atmosphere-land-water system and long-term changes in climate has generated proposals for new types of remote sensing systems, including hyperspectral sensors. Hyperspectral sensors combine spatial (imaging sensor) and spectral (spectrometer) resolution in a single data set. The only abundant source of such data to date has been the JPL AVIRIS system. In the visible spectral region, the atmosphere can provide half or more of the total signal seen by the sensor at altitude. In conjunction with ground measurements at relatively high reflectance targets and LOWTRAN models, calibrated AVIRIS radiance data near 870nm and 940nm has been used to produce spatial maps (at 40m x 40m resolution) of total precipitable water vapor over 300km2 areas (Conel, et al, 1988).

It is also possible to derive estimates of aerosol properties from visible and near IR sensor-measured radiances. The signal (in this case, non-reflected component of the upwelling radiance) is best measured over low reflectance targets, such as water bodies. Such atmospheric measurements, in addition to their intrinsic scientific merit, are useful for calibration of radiative transfer codes used in the analysis of hyperspectral imager data. Remote sensor calibration is particularly important in oceanographic applications (Gordon, 1981; Gordon, et al, 1983) where signal (in this case, surface and near-surface reflectance) levels are characteristically low.

New sensors, such as the Navy HYDICE system, will provide high spectral (on the order of 10nm) and spatial (on the order of 3m) resolution over the spectral range 0.4 to 2.4 mm, with a SNR that is an order of magnitude higher than that of AVIRIS. The relatively high SNR of HYDICE in the water vapor absorption bands near 0.9 and 1.1 mm should permit high quality atmospheric retrievals of water vapor. At other wavelengths, the quality of the HYDICE sensor should result in valuable information on atmospheric aerosols and other constituents, land and ocean properties, that can serve as input to atmospheric and climate models.

The remainder of Section 1 consists of an introduction to MIS, Version 3.0, and Sections 2 and 3 discuss its use in sensor imaging simulation, while Section 4 presents some simulation examples.

1.1 Multispectral Image Simulator 3.0

MIS 3.0 is a software system to simulate the performance of satellite or aircraft-based imaging. With MIS 3.0, an imaging system response can be investigated using a given ground reflectance database or a simulated ground reflectance. MIS 3.0 is based on codes of SADIE (System at Arizona for Digital Image Experimentation) for image processing tools and 5S (Simulation of the Satellite Signal in the Solar Spectrum) to estimate the signal measured by a satellite sensor due to solar radiation reflected and scattered upward by the surface-atmosphere system. MIS integrates aspects of individual remote sensing processes and presents the final images.

MIS 3.0 is written and compiled under SunOS. Section 2 describes the basic principles behind the modelling of the atmosphere effect and the system response. Section 3 introduces the use of the MIS software, through the text menu. Section 4 describes applications of the software.

Throughout the report, a *directory* will be printed in italic, a **filename** in bold, and an ***executable*** file in bold and italic

4

2.0 SYSTEM MODELING AND SIMULATION

The simulation of the remote sensing system involves a calculation of the radiance that the sensor receives and the conversion of that radiance onto digital numbers through the imaging system. The basis of this radiance calculation is the 5S program.
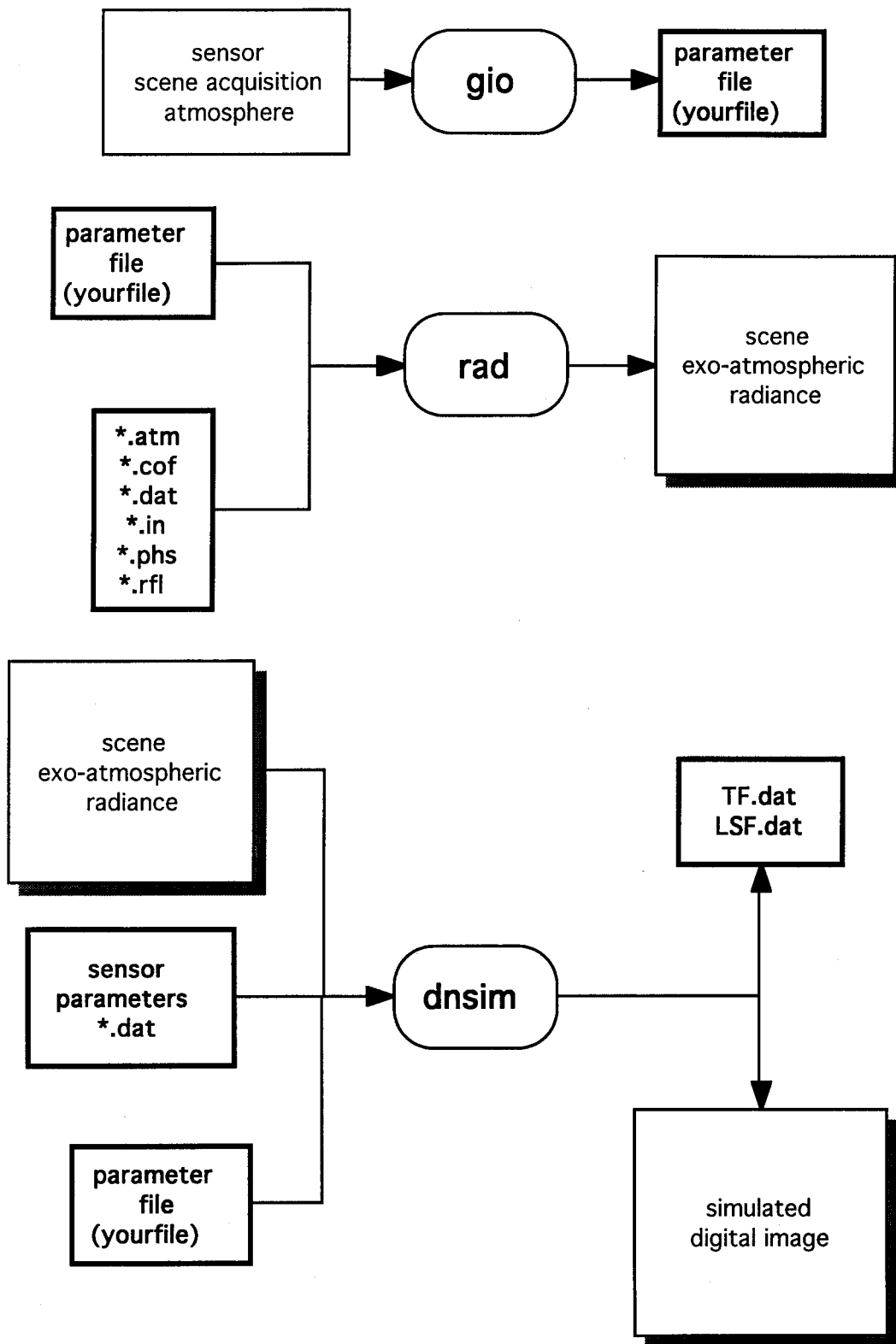
Figure 1. Block Diagram of the MIS 3.0 Program

2.1 Scene modeling

To calculate the above-the-atmosphere (exo-atmospheric) radiance corresponding to a certain ground reflectance value, several parameters are needed. The solar irradiance, angle between the irradiance source and the imaging sensor, reflectance value, atmosphere condition, and spectral band are necessary parameters. 5S incorporates all of those parameters into one single apparent reflection, ρ^*. Based upon this apparent reflection, the radiance image on the entrance pupil of the sensor is then calculated using :

$$L = \rho^* \cdot E / \pi$$

where E is the solar irradiance that illuminates the reflectance map (or simulated reflectance map). Thus, the following are assumed:

The surface exhibits Lambertian reflectance and
The topography is flat

An example of a typical radiance simulation parameter set is shown in Table 1. The parameter values shown here will be used later in simulated image performance (Section 4).

```
===================================================================
        Table 1. Radiance Simulation Parameters (file: hydice_parameters.dat)
-------------------------------------------------------------------
*** Sensor type and geometrical parameters ***

8                   (sensor:HYDICE)
8/23                (month/day)
11.200000           (time)
14.000000           (altitude (km))
40.000000           (solar azimuth)
30.000000           (solar zenith)
0.000000            (sensor azimuth)
0.000000            (sensor zenith)

***  Sensor band filter ***

1                   (band filter:Uniform Band Filter)
0.450000            (min wl)
0.460000            (max wl)

***  Atmospheric absorption model   ***

1                   (Tropical Profile : (H2O = 4.120 G/CM2, O3 = 0.247 CM-
ATM))

*** aerosol model ***

2                   (Maritime Model)
40.000000           (visibility[km])

*** Only for pixel array simulation use ***

0.000000            (target elevation [km])
0.200000            (target  radius [km])
3                   (block window size)
===================================================================
```

2.2 Sensor modeling

The HYDICE system has the following parameters:

Total MTF:	Gaussian (0.25 @ 0.5 cycle/pixel) [1]
IFOV	500 μrad [1]
Altitude	0 - 14.000m, 6000m typical [1]
Quantization	12 bits [2]
Spectral Channels	210 (0.4 - 2.5 μm) [2]

(These spectral channels are divided into the 3 units for modeling purposes: [3]

Channel A : 0.4 - 1.0 μm

Channel B : 1.0 - 1.9 μm

Channel C : 1.9 - 2.5 μm)

Jitter   44 urad [4]

Since HYDICE can operate at different altitudes, its ground IFOV can vary:

$$\text{Ground IFOV} = \text{IFOV(rad)} \cdot \text{altitude}$$

An example of a typical HYDICE Parameter Specification set is shown in Table 2.

===
Table 2. HYDICE Parameter Specification

```
0.25       /* optics MTF: 0.25 at 0.5 cycle/pixel 5           */
3          /* F number 2                                      */
27         /* aperture (mm) 2                                 */
40         /* slit (μm) 6                                     */
0.028      /* Velocity to Height ratio (rad/s) 1              */
40         /* detector size cross track (μm) 2                */
40         /* detector size along track (μm) 2                */
12         /* number of bits/pixel                            */
10400000   /* full well electron number of Channel A          */
6600000    /* full well electron number of Channel B          */
2200000    /* full well electron number of Channel C          */
0          /* offset of DN at zero electron number            */
10.5       /* detector integration time (ms)                  */
8.73e-14   /* dark current (electron number)                  */
1102.0     /* detector read out noise Channel A (electron number) 7  */
668.0      /* detector read out noise Channel B (electron number)    */
272.0      /* detector read out noise Channel C (electron number)    */
0.0        /* electronics (signal chain) noise : electron number 8   */
```
===

---

[1] Basedow, et al (1992), Table 1

[2] Basedow, et al (1992), Table 2

[3] Rappoport, et al (1994), Table 3

[4] e-mail note from Bob Basedow, HDOS

[5] Rappoport, et al (1994), Table 1

[6] Basedow, et al (1992), Figure 7

[7] Rappoport, et al (1994), Table 3

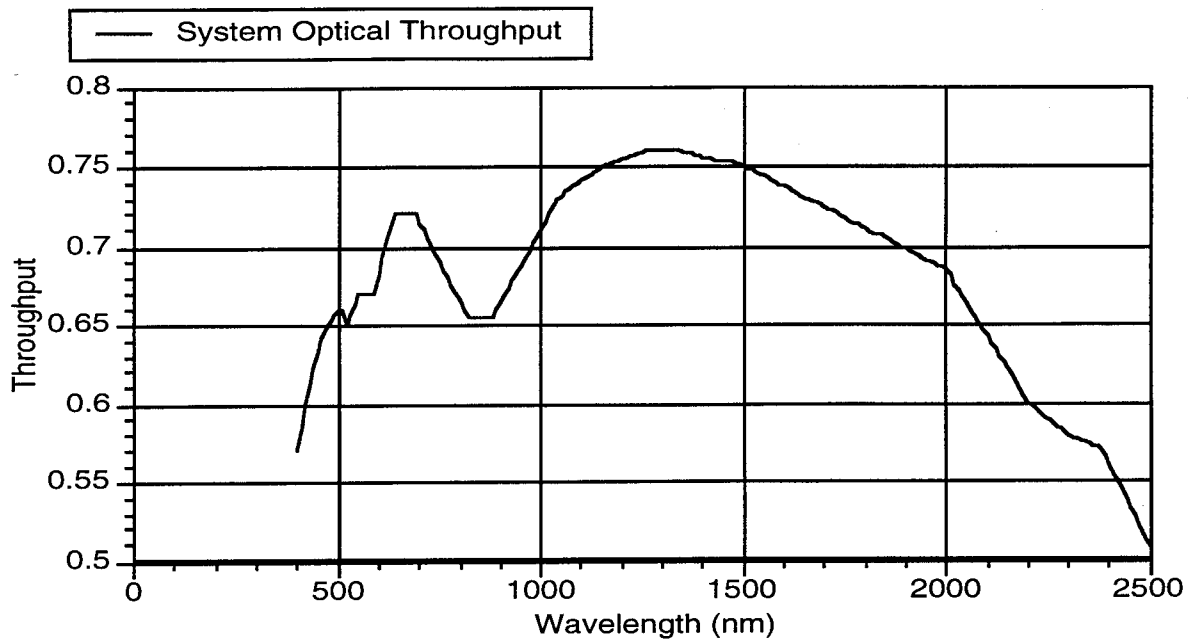[8] Undefined, assumed zero

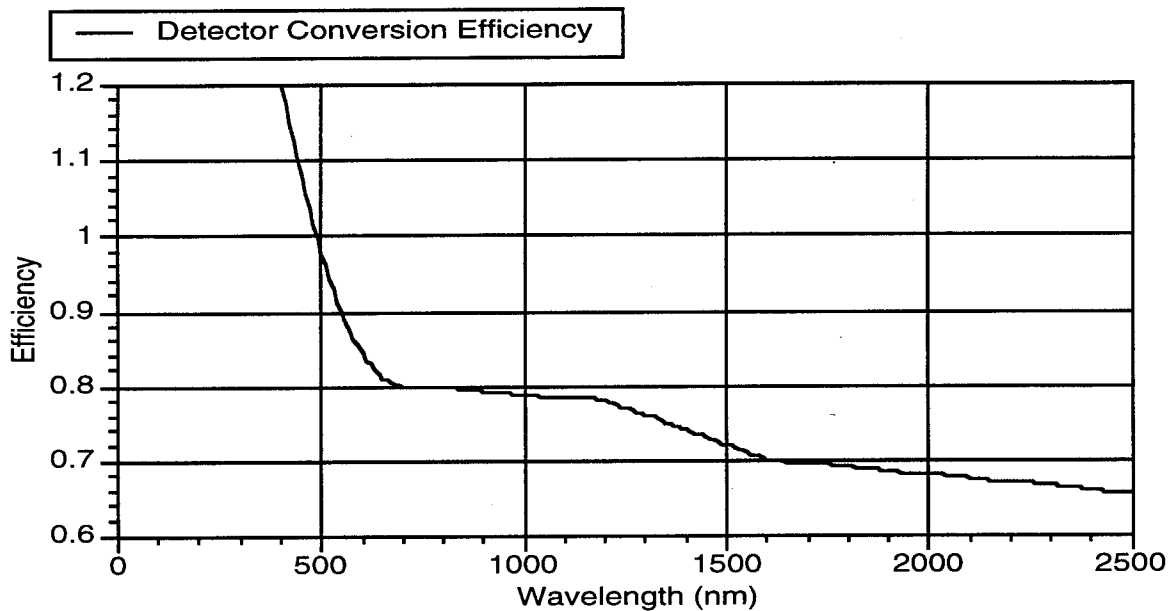Figure 2. System Optical Throughput of HYDICE (Basedow et al, 1992)

Figure 3. Measured Detector Conversion Efficiency of HYDICE (smoothed version of Figure 3, Basedow et al (1992))
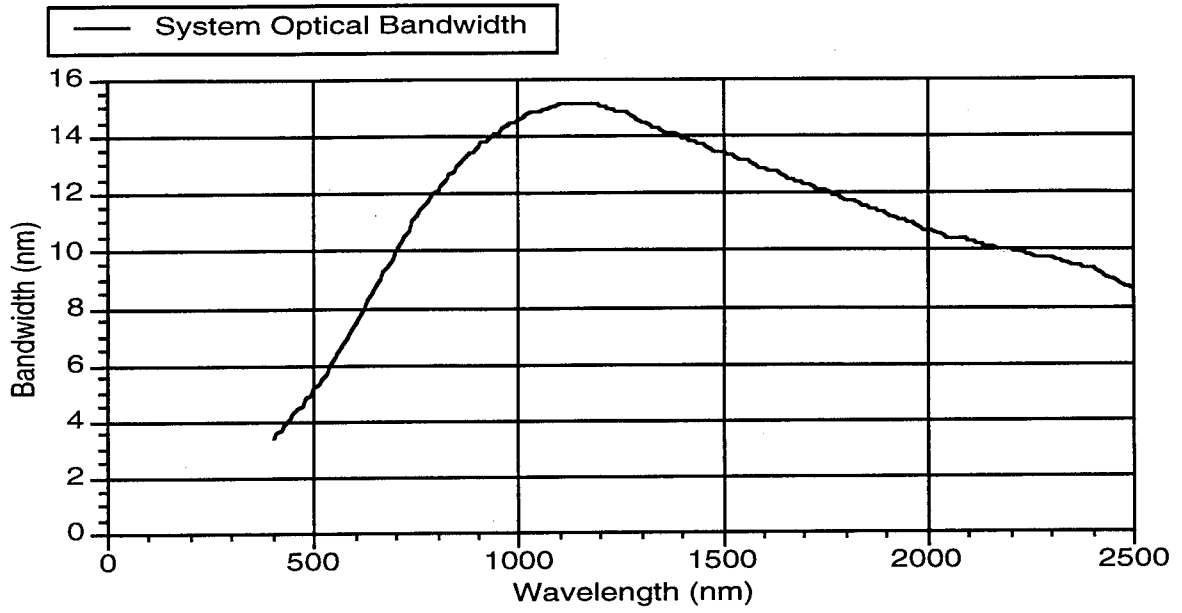
Figure 4. Channel bandwidth of HYDICE without band averaging below 600nm (Basedow et al, 1992)

3.0 GETTING STARTED WITH MIS 3.0

3.1 Installing MIS 3.0

To install MIS 3.0, you have to have at least 35MB of hard disk space for all the final files including the database; this does not include disk space needed to compile or execute the software. A makefile program and a C compiler are also needed; three 'makefile' sources called **m-gio**, **m-rad**, and **m-dnsim** are included for compiling with cc in SunOS. These files are located in the working directory.

The following subdirectories should be included in one working directory (the directory names are listed in the file **filelist**) :

> *./cup_refl*
> Contains a database of Cuprite, Nevada, area reflectance map. The images are in SADIE format with 20m/pixel sample interval.

> *./data*
> Contains transfer function (TF) and line spread function (LSF) of the optical system, generated from sensor modelling

> *./images*
> Contains images created by *rad* and *dnsim*

> *./infile*
> Contains data files for atmospheric simulation and imaging sensor parameter (F–number, focal length, etc). The following are the extensions used:

> | | |
> |---|---|
> | **.atm* | : atmospheric models for specified region and season (Midlatitude winter model, Tropical model, etc). Contains H2O & 03 concentration, pressure, and temperature as a function of altitude. |
> | **.cof* | : coefficient files for gaseous transmission model |
> | **.in* | : input file for atmosphere absorption and scattering model |
> | **.phs* | : aerosol basic components |
> | **.rfl* | : reflectance of specific ground cover types (vegetation, sand, etc) |

> *./pin*
> Contains parameters for different sensor systems. The files are created by *gio*.

> *./src*
> Contains MIS library and source code, and object code generated by SADIE.

> *./sadie-v4.2* (optional)
> Contains SADIE source code and its makefile called **m-sadie**.

To generate the executable files under SunOS (or any Unix OS), execute:

```
make -f m-gio
make -f m-rad
make -f m-dnsim
```

After the corresponding makefiles are compiled, three executable files are produced: *gio*, *rad*, *dnsim*. If you would like to execute it under a different operating system, you have to recompile the SADIE files by executing

```
make -f m-sadie
```

under the directory *./sadie-v4.2* . The resulting file, **libsadie.a** should then be moved to the directory *./src* before compiling *gio*, *rad*, or *dnsim*.

Note that any extension of a command line inside a bracket such as [-f filelist] is optional.

3.2 *gio* : Creating Parameter File

Before we start doing any simulation, an imaging condition parameter file has to be created by using *gio*. The syntax is

gio [-i namelist] [-f filelist] geo_file

where

namelist:	file that contains all input parameters needed
filelist:	file that contains a list of all of the directories, relative to the current directory
geo_file:	file created by *gio*. It contains sensor type, atmospheric conditions, and simulation conditions.

The format for filelist is:

dir1 (directory for AVIRIS Cuprite reflectance database)
dir2 (directory for Transfer Functions and Line Spread Functions created by *rad* and *dnsim*)
dir3 (directory for images created by *rad* and *dnsim*)
dir4 (directory for data files and sensor parameters)
dir5 (directory for local-condition file created by *gio*)
dir6 (directory for bandspectrum)

For example, the contents of our filelist is as follows:

cup_refl
data
images
infile
pin
specband

Note that *rad* and *dnsim* also use [-i namelist], [-f filelist], and geo_file.

gio will automatically save the parameters inside geo_file, and it will be saved under subdirectory *./pin*. This file will then be used as an input for *rad* and *dnsim*. The following parameters should be specified:

• Sensor specification:

  • Sensor Type (e.g. Meteosat, GOES, HYDICE ...)
  • Month, Day, Time, Altitude, Solar and Sensor zenith and azimuth
  • Spectral Band of the sensor
  • Range of Wavelengths to be simulated

• Atmospheric specification:

  • Atmospheric Absorption Model (amount of H_2O and O_3 as given by the general temperate zone Tropic, SubTropic ...)
  • Aerosol Model (amount of Dust-like, Water-Soluble, Oceanic, Soot as given by the general location Continent, Urban...)
  • Visibility

• Target specification:

  • Target Elevation (average elevation of the map used as reflectance map)
  • Target Radius
  • Block size (specifies the effective range of neighboring radiance, i.e. the adjacency effect)

Note that in our geo_file, times are in decimal fractions and all angles are in degrees. Azimuth is relative to the north direction and zenith is relative to the normal vector.[9] Northern latitude is positive and Eastern longitude is 0 - 180 degrees whereas Western longitude is 180 - 360.

An example of using *gio*:

$$gio \text{ -i } \textbf{keys -f dirs hiris.gio}$$

3.3 *rad*: Converting Reflectance Map to Radiance Image

rad is used for simulating the scene spectral radiance, which is the radiance at the height of the sensor. It takes the output generated by **gio** and all the information regarding the system to be simulated. The command line is:

$$rad \text{ [-i namelist] [-f filelist] [-e] [-h] [-p] [-x] geo\_file}$$

with options:
    -e = external database
    -h = output in HDF file format
    -p = irradiance at a single pixel computation
    -t = test case, to see what reflectance images are needed
    -x = test mode

---

[9] In the version of MIS supplied to SAIC for littoral simulation, the format for azimuth (ϕ_S) must be changed to be relative to the wind direction for compatibility with Dr. Curt Mobley's Hydrosol code.

Default is to do array (image) computation and save the output in SADIE format.

geo_file is the file created by *gio* . Based on a given database, this program will compute a radiance image for the specified range. Depending on the sensor type, *rad* can either do a radiance integration or interpolation. For example, if TM1 is specified, then *rad* will use the reflectance maps with wavelength between 0.43um and 0.55um for radiance integration.

A database for this purpose is located in *./cup_refl*. It contains images of Cuprite, Nevada, derived from AVIRIS images by the USGS. It has a spectral resolution of 10nm and spatial resolution of 20m, with size of 400 lines x 410 pixels. Since the 5S program has a resolution of 5nm, the database will be interpolated in wavelength.

If you choose to use an external database with -e option, the program will prompt you to enter the filename for each reflectance images needed. The image spectral resolution has to be 10nm, and in HDF format. To check how many images are needed and at what wavelength, use -x option.

If only a single pixel is to be computed, the following parameters have to be specified:

• Target Type (Reverse Run, Homogeneous or Non-Uniform Ground)

• Target Ground Reflectance (Constant, Spectral Vegetation, Sand, etc)
    Can be uniform (single type) or non uniform (multi type).

• Environment Ground Reflectance (Constant, Spectral Vegetation, Sand, etc)
    Can be uniform (single type) or non uniform (multi type).

With this choice, the program will calculate the irradiance value at the ground and at the specified sensor height based on given reflectance value, and then print those values.

For pixel array simulation, the program will compute the radiance at specified wavelengths based on the image reflectance map database, and then save it as an irradiance image map for future use with *dnsim*.

3.4 *dnsim*: Conversion of Radiance to Digital Number

dnsim is used for simulating the digital image produced by the sensor. The command line is:

> *dnsim* [-i namelist] [-f filelist] [-p] [-h] geo_file

where **geo_file** is the parameter file created by *gio*. Then the program will prompt the user to select one of the following input radiance sources:

• Input radiance
    Use this option to simulate a digital image using the radiance image map created by *rad*.

• 1D or 2D image sinewave

14

Use this option to create a sinewave image with a specified size, period, minimum and maximum reflectance. Note that the specified period is for the sample increment, not the ground increment for the sensor.

- Patch image
  This will create a square image on top of a background.

To simulate a 1-D sinusoidal image seen by the HYDICE sensor, we have to know both the sampling increment and the sensor ground increment. For example, to simulate a sinusoidal sensor image with a period of 0.1 cycle/pixel given that the sampling increment is 3.5m and the sensor height is 14km, then the period entered should be:

$$14000 * 0.5*10^{-3} / (3.5 * 0.1) = 20$$

where $0.5*10^{-3}$ = HYDICE IFOV (rad)

After input selection, the next step is image sensor selection:

- Image Sensor Selection
  Choosing a sensor. Default is whatever is supplied by your file

- MTF Calculation Setting
  Changing sampling parameters. Change this if your database resolution or simulated radiance image resolution is different from the default value (3.5m for HYDICE)

- Start the MTF Computation
  This will calculate the coefficients needed to compute the spatial degradation. All files will be saved under directory *./data*. Those files are:
  alongTF.dat
  alongLSF.dat
  crossTF.dat
  crossLSF.dat

The following will appear only after MTF/LSF have been calculated:

- Print Sensor MTF/LSF
  Print along/cross–track MTF or LSF for the system

- Image Simulation
  Simulate digital number (DN) using sensor TF and simulated radiance image, or using image radiance created with *rad* from database. Will use the test radiance image created at the beginning of *dnsim* execution or prompt the users to enter a radiance image file created by *rad*. By selecting this choice, the program will convert the radiance image into electron number and then sample it to create a simulated digital image as in the actual system.

- Target Simulation
  Used as an alternative for SNR investigation.

If an image simulation is done, the following images are created:

15

rad   Image of exo-atmospheric radiance at the system altitude

irr   Image of input irradiance on the system after losses in the system

blurr   Image of input irradiance after blurring by optics

det   Image of electron number per pixel after conversion from photon by detector

EltNoise Image of electron number per pixel after the addition of noises

DN   Digital image from detector; range depends on the number of bits/pixel used in the system

Sampled Downsampled digital image to achieve the resolution of the system

The filename extension depends on the file format used.

4.0 IMAGE SIMULATION USING MIS3.0

Here, two application examples are presented to demonstrate the possible use of MIS 3.0 in HYDICE system simulation.

4.1 Sinewave Image Performance

As the irradiance image passes through the imaging system and is converted into a digital number (DN), noise will be added to the final output by various stages in the imaging system. The total system performance can be measured with the output signal–to–noise ratio (SNR). The equation is:

$$\text{output SNR} = 20 \log[DN_{pp}/(\text{sum of all noise variances})^{1/2}]$$

where DN_{pp} is the peak–to–peak difference in the output DN. To simulate a spatially–varying scene, we can generate a 1–dimensional sinusoidal image and pass it through the imaging system. For this purpose, a radiance parameter file as in Table 1 has to be created using *gio*. The next step is to use this file as an input to *dnsim*.

As you run *dnsim*, the program will prompt you to choose the input mode. To evaluate the effect of the imaging system on SNR, the user can create sinusoidal images with different frequencies and reflectance values. Here, the test conditions are:

• Three different maximum reflectances, 0.06, 0.07, and 0.08, with the same minimum reflectance of 0.05 to represent clear water. This results in reflectance differences ρ_{pp} of 0.01, 0.02 and 0.03, respectively.

• Three different spatial frequencies of 0.1, 0.2, and 0.4 cycle/pixel

• Three different wavelengths 455, 1950, and 2300 nm to represent different channels

Because we have to do three separate tests for each channel A, B and C, the total number of reflectance images created is 27. In the following graphs, an input SNR is given for each case, which represents the peak–to–peak electron signal divided by the standard deviation of the shot noise.
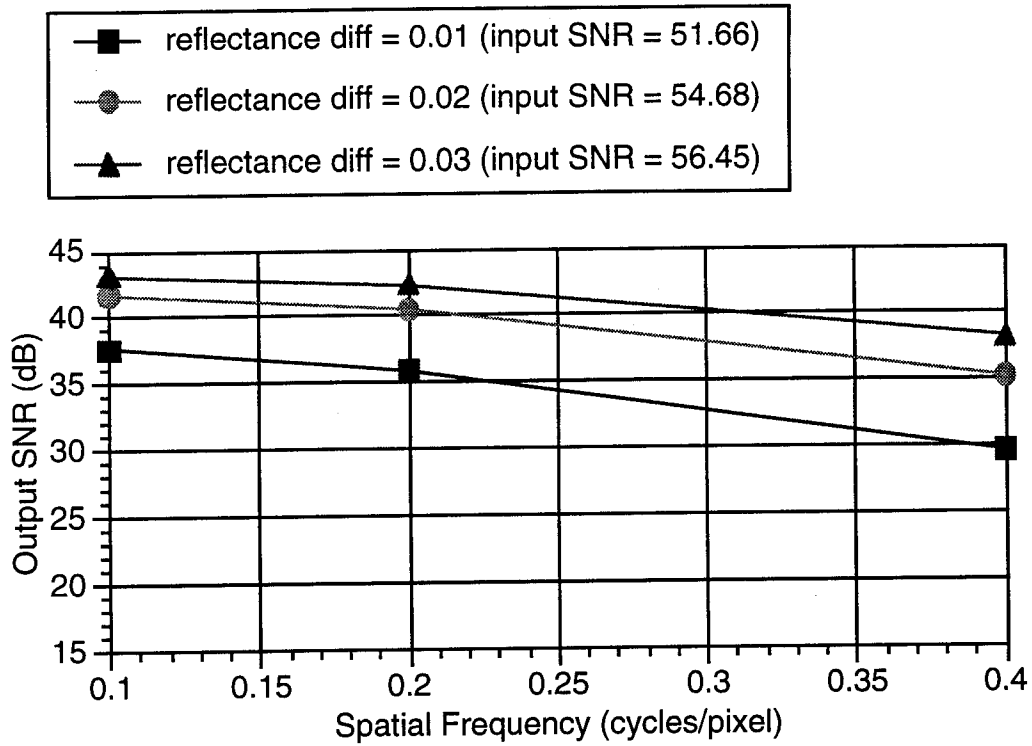
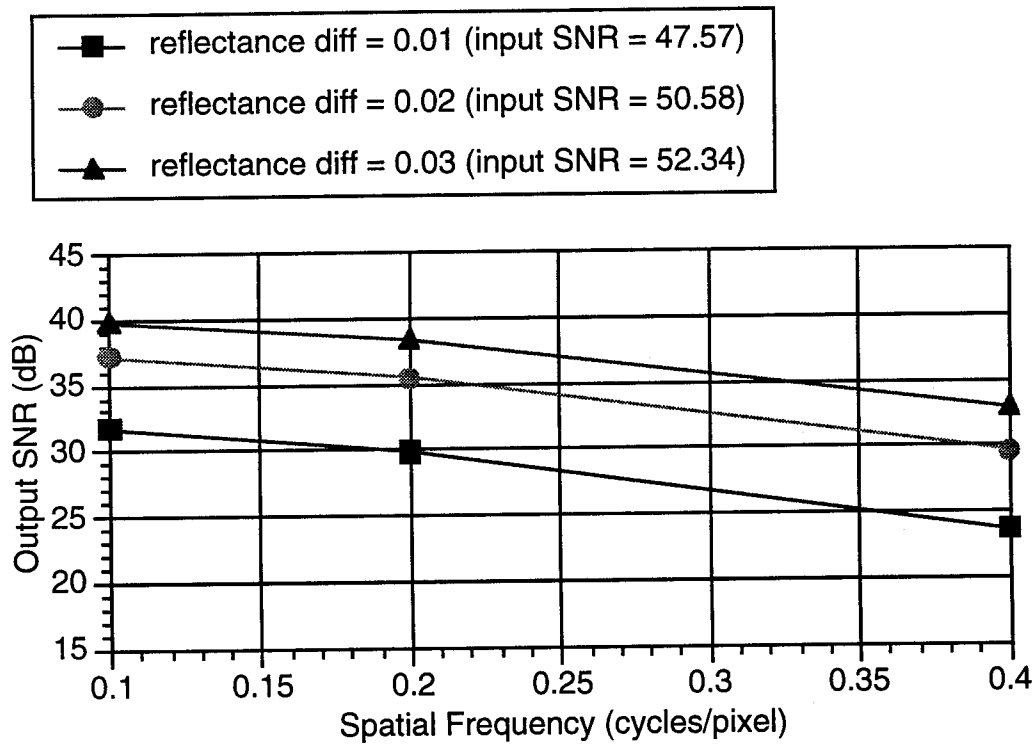Figure 5. SNR in Channel A, wavelength = 455 nm

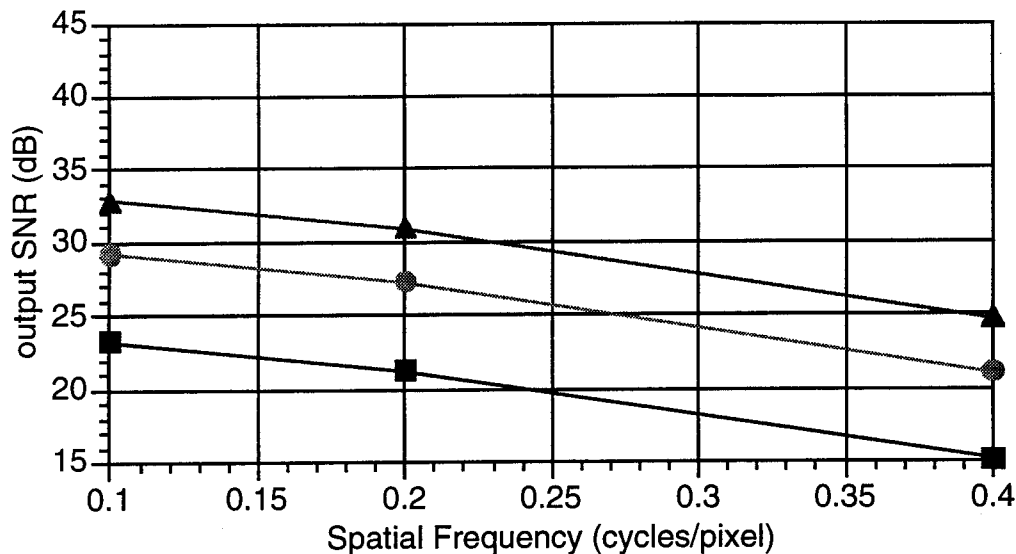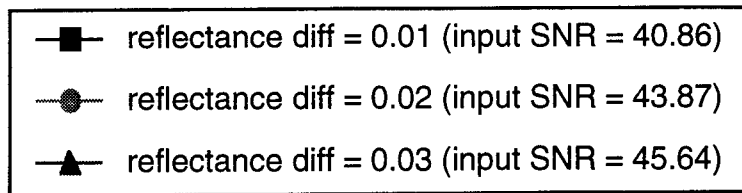Figure 6. SNR in Channel B, wavelength = 1655 nm

Figure 7. SNR in Channel C, wavelength = 2155 nm

Several common features in the results of this simulation are immediately apparent. For the same ground reflectance, but different radiance wavelengths, SNR inputs are different. The input SNR at 455 nm is 4.09 db higher than at 1655 nm, and 10.8 db higher than at 2155 nm. For all wavelengths and ground reflectances, as the input frequency increases, the output SNR decreases. This shows that the degradation introduced by the system increases as the input spatial frequency increases due to the sensor MTF.

4.2 Simulated Natural Image Performance

For a study of the effects of atmospheric absorption and scattering and the imaging system, the database image of Cuprite, Nevada is used. First, a file as shown in Table 3 is created using *gio*. Then, *rad* is used to form a radiance image at the sensor altitude.

19

```
================================================================================
                      Table 3: The Parameters used for Image Sensing Test
--------------------------------------------------------------------------------
*** Sensor type and geometrical parameters ***

8                       (sensor:HYDICE)
12/2                    (month/day)
11.200000               (time)
14.000000               (altitude (km))
0.000000                (solar azimuth)
20.000000               (solar zenith)
120.000000              (sensor azimuth)
30.000000               (sensor zenith)

***  Sensor band filter ***

1                       (band filter:Pixel Array)
0.450000                (min wl)
0.460000                (max wl)

***  Atmospheric absorption model   ***

1                       (Tropical Profile : (H2O = 4.120 G/CM2, O3 = 0.247 CM-
ATM))

*** aerosol model ***

1                       (Maritime Model)
50.000000               (visibility[km])

*** Only for pixel array simulation use ***

1.000000                (target elevation [km])
0.020000                (target  radius [km])
3                       (block window size)
================================================================================
```

dnsim then uses this parameter file, sensor parameter file, and radiance image created by *rad* to simulate the effect of the sensor. Note that HYDICE has a higher resolution (7m or less) compared to the Cuprite reflectance image database created by AVIRIS (20m). We therefore use this image database and assume that it has a 3.5m resolution. The resulting HYDICE simulated images are not absolutely realistic because of this assumption, but are relatively realistic compared to the input scene.

```
==========================================================================
                        Table 4: The Output of dnsim
--------------------------------------------------------------------------
Radiance before system lossess:
        max  = 0.180992
        min  = 0.067399
        diff = 0.113593
Input irradiance :
        max  = 0.015795
        min  = 0.005882
        diff = 0.009913

Input irradiance after system lossess (mW/cm^2):
        max  = 0.010001
        min  = 0.003724
        diff = 0.006277

Cross filtering .. please wait ..


Along filtering .. please wait ..


Blurred irradiance (mW/cm^2):
        max  = 0.009279
        min  = 0.003985
        diff = 0.005295

Detector output in number of electrons:
        max  = 3849418.5
        min  = 1653041.4
        diff = 2196377.1

Input  SNR = 65.815414 (dB)
Output SNR = 171.971 (44.71 dB)

Simulate shot noise and read noise..

Electronic + noise in e-
        max  = 3851438.5
        min  = 1655595.4

Signal scaling and A/D conversion ..

DN image
        max  =    1516
        min  =     651

Sampled DN
        max  = 1491
        min  =  653
==========================================================================
```
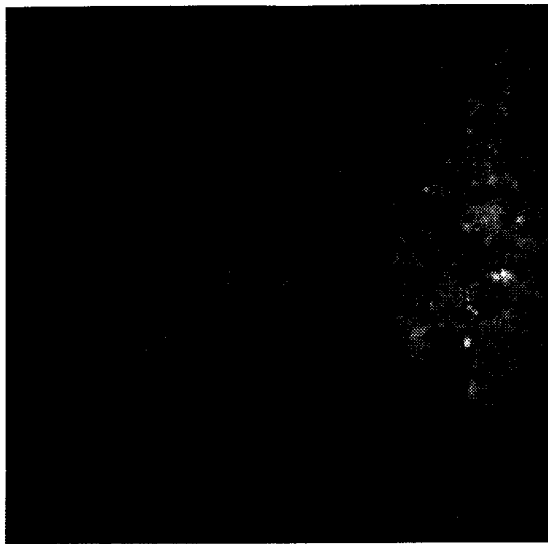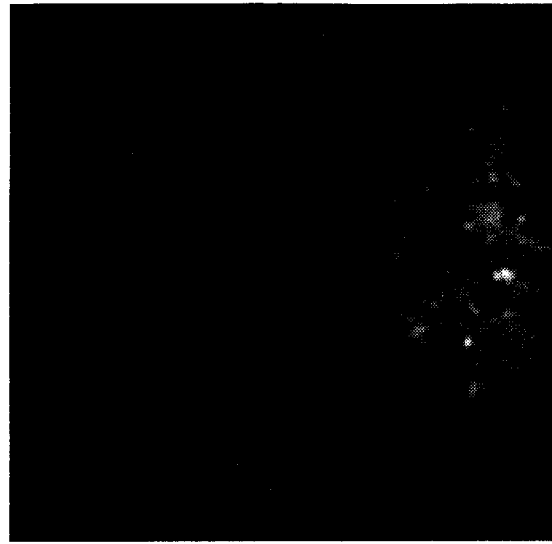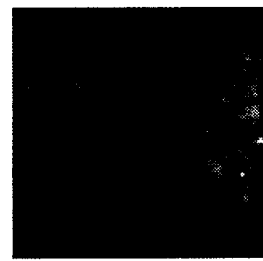
Irradiance image

Blurred image

Blurred image with noise

Sampled image

Figure 8: Images generated by *dnsim*

The final simulated image is smaller than the one we start with because the database ground resolution is assumed to be 3.5m and the HYDICE ground resolution is assumed to be 7m. To achieve the desired resolution, the simulated image is down sampled (the above sampled image has also been trimmed in area slightly).

4.3 Simulation of the Effect of Scan Angle

The effect of scan angle on the image formation was also studied using MIS 3.0. Using simulation, we would like to see the relationship between scan angle and the radiance received. Simulated images of a 1-D sinusoidal target, size 100x100 pixels, with a spatial frequency of 0.2 cycle/pixel, were created. The following are the input parameters needed (created using *gio*) :

```
=====================================================================
*** SENSOR TYPE, TIME, AND GEOMETRIC PARAMETERS ***

3                   (sensor:AVHRR (NOAA8))
2/11                (month/day)
19.500000           (time)
860.000000          (altitude (km))
1024                (pixel)
-108.500000         (ascendant node logitude)
19.5000000          (ascendant node overpass time)

***  Sensor band filter ***

3                   (band filter:AVHRR (NOAA8) 1)


***  Atmospheric absorption model    ***

1                   (Tropical Profile : (H2O = 4.120 G/CM2, O3 = 0.247 CM-
ATM))

*** aerosol model ***

2                   (Maritime Model)
23.000000           (visibility[km])

*** Only for image simulation use ***

0.000000            (target elevation [km])
0.500000            (target  radius [km])
3                   (block window size)
=====================================================================
```

Here, AVHRR sensor was chosen because its large scan angle ($\pm 54^\circ$) will better illustrate the scattering effect. The geographical area is near Hawaii in the Pacific Ocean. Note that the ascendant node is more than 180° because it is located at a Western longitude. MIS 3.0 will directly compute the latitude and longitude of the specified pixel position (between 0 and 2048 since AVHRR only has 2048 pixels per line), and the local time and the solar location. Pixel 1024 is at the center of swath. Based on this result, MIS will then simulate the image created by AVHRR. To get the image at different pixel locations, the above file was edited to change the pixel number. (Note, this simulation currently uses the parameters for only the single pixel at the specified scan angle, which is at the center of the 100x100 pixel target. These parameters are then assumed to apply to all pixels in the target, which is equivalent to an assumption that the target size is small relative to changes in the simulated quantity, irradiance versus scan angle). The simulation is computed at 10 different pixel positions: 0, 256, 512, 640, 768, 1024 (nadir), 1280, 1536, 1792, and 2048 cross–track.
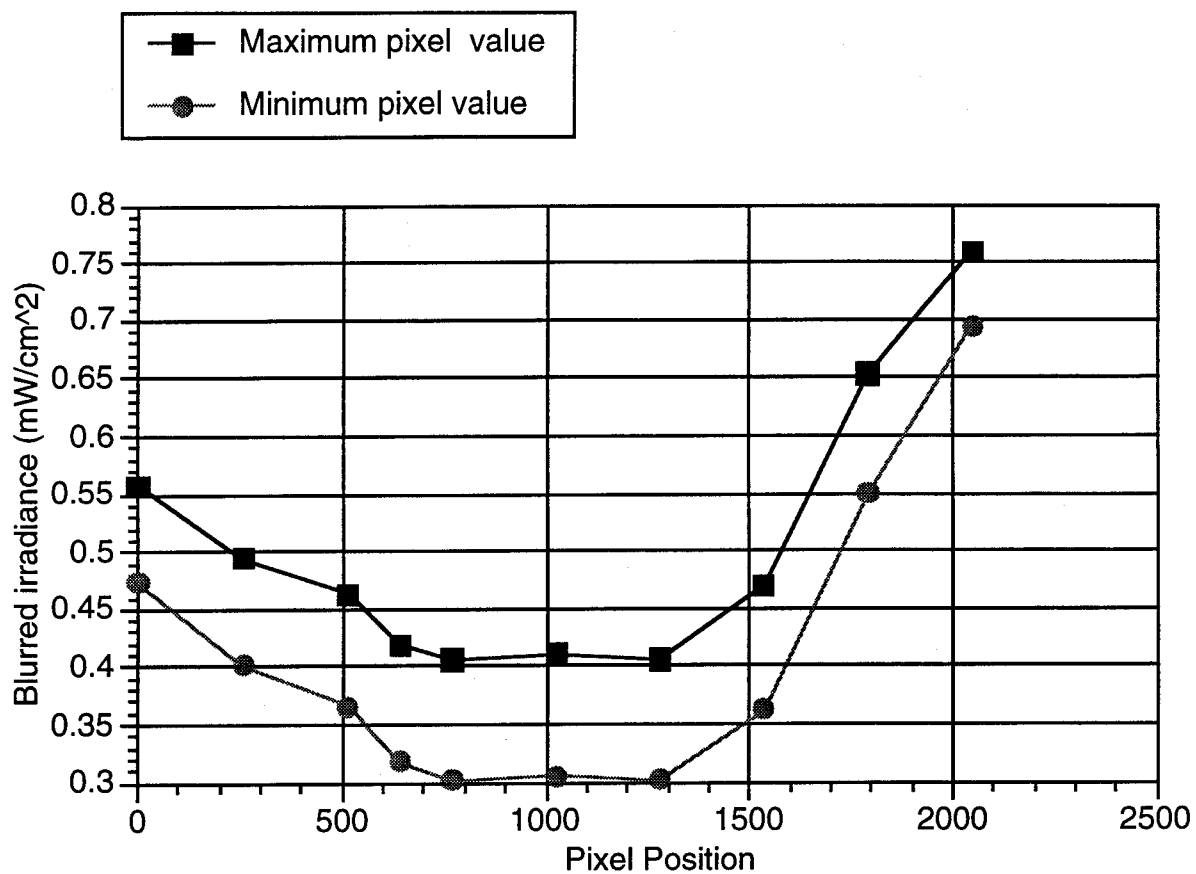
Figure 9. Viewing angle effect on the sensor focal plane irradiance (AVHRR simulation)

From the center pixel position, as the scan angle increases, the maximum and minimum pixel values in the blurred image decrease due to the increased direct path between the sensor, ground, and the sun. However, as the scan angle increases more for pixel positions greater than 1280 or less than 768 (corresponding to scan angles greater than 16.5°) the pixel values increase sharply due to the effects of scattering. In general, the final simulation result is consistent with actual AVHRR imagery [Duggin and Piwinski, 1992].

5.0 References and Bibliography

Basedow, R., P. Silverglate, W. Rappoport, R. Rockwell, D. Rosenberg, K. Shu, R. Whittlesey, and E. Zalewski, "The HYDICE Instrument Design," *Proc. of the Int. Symposium on Spectral Sensing Research,* vol 1., pp. 430-445, 1992

Conel, James E., Robert O. Green, Veronique Carrere, Jack S. Margolis, Ronald E. Alley, Gregg Vane, Carol J. Bruegge and Bruce L. Gary, "Atmospheric Water Mapping with the Airborne Visible/Infrared Imaging Spectrometer (AVIRIS), Mountain Pass, California," *Proc. of the Airborne Visible/Infrared Imaging Spectrometer (AVIRIS) Performance Evaluation Workshop,* June 6-8, 1988, JPL Publication 88-38, Jet Propulsion Laboratory, Pasadena, California

J. Duggin and D. Piwinski, "Scan Angle Dependence of Radiance recorded by the NOAA-AVHRR," *Proc. SPIE Advanced Remote Sensing,* no. 363, p. 98-103, 1992

Gordon, H. R., "Reduction of Error Introduced in the Processing of Coastal Zone Color Scanner-type Imagery Resulting from Sensor Calibration and Solar Irradiance Uncertainty," *Applied Optics,* Vol. 20, p. 207, 1981.

Gordon, H. R., D. K. Clark, J. W. Brow, O.B. Brown, R.H. Evans, and W. W. Broenkow, "Phytoplankton Pigment Concentrations in the Middle Atlantic Bight: Comparison of Ship Determinations and Satellite Estimates," *Applied Optics,* Vol. 22, P. 20, 1983.

P. Kerekes and D.A. Landgrebe, *Modelling, Simulation, and Analysis of Optical Remote Sensing Systems,* School of Electrical Engineering, Purdue University, 1989

Leroy and J.-L. Roujean, "Sun and View Angle Corrections on Reflectance Derived from NOAA / AVHRR Data," *IEEE Trans. on Geoscience and Remote Sensing,* vol. 31, no. 4, pp. 764-770, 1993

W. Rappoport , R. Basedow, P. Silverglate, E. Zalewski, D. Gulbransen, C. Peterson, J. Rosbeck, L. Ruzicka, D. Murphy and R. Wyles, *HYDICE Focal Plane Design and Performance,* Hughes Danbury Optical Systems, Inc., 1994

D. Tanre and et al., *Simulation of the Satellite Signal in the Solar Spectrum (5S).* Laboratoire d'Optique Amospherique, France, 1987

H-H. Wu and R.A. Schowengerdt, *Multispectral Imaging Simulator (MIS) Version 1.0.* DIAL Lab, Electrical and Computer Engineering, Univ. of Arizona, 1991

H-H. Wu and R.A. Schowengerdt, *Multispectral Imaging Simulator (MIS) Version 2.0. User Manual* DIAL Lab, Electrical and Computer Engineering, Univ. of Arizona, 1991